Quasi-Elastic Light Scattering of Platinum Dendrimer-Encapsulated Nanoparticles

Christina H. Wales,[†] Jacob Berger,[‡] Samuel Blass,[‡] Richard M. Crooks,[*,†] and Neer Asherie[*,‡]

[†]Department of Chemistry and Biochemistry, Texas Materials Institute, Center for Nano and Molecular Science and Technology, The University of Texas at Austin, 1 University Station A5300, Austin, Texas 78712, United States

[‡]Department of Physics and Department of Biology, Yeshiva University, New York, New York 10033, United States

ABSTRACT: Platinum dendrimer-encapsulated nanoparticles (DENs) containing an average 147 atoms were prepared within sixth-generation, hydroxyl-terminated poly(amidoamine) dendrimers (G6-OH). The hydrodynamic radii (R_h) of the dendrimer/nanoparticle composites (DNCs) were determined by quasi-elastic light scattering (QLS) at high (pH ~10) and neutral pH for various salt concentrations and identities. At high pH, the size of the DNC (R_h ~4 nm) is close to that of the empty dendrimer. At neutral pH, the size of the DNC approximately doubles (R_h ~8 nm) whereas that of the empty dendrimer remains unchanged. Changes in ionic strength also alter the size of the DNCs. The increase in size of the DNC is likely due to electrostatic interactions involving the metal nanoparticle.
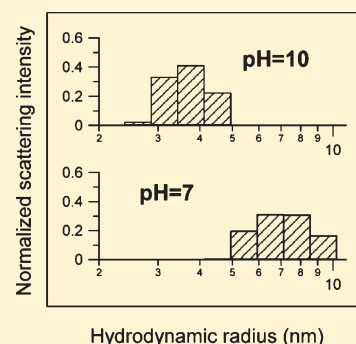
■ INTRODUCTION

One of the principal methods of producing nanoparticles is by the reduction of metal ions within dendrimers.[1] Monometallic,[2−8] alloy,[5,8,9] and core/shell[5,9] bimetallic dendrimer-encapsulated nanoparticles (DENs) have been synthesized and characterized by our group[5] and others.[10−12] Platinum DENs are synthesized in a two-step process. First, $PtCl_4^{2-}$ is added to an aqueous solution of sixth-generation, hydroxyl-terminated poly(amidoamine) (PAMAM) dendrimers (G6-OH). This yields the DEN precursor G6-OH($Pt^{2+})_n$, where Pt^{2+} refers to any form of Pt^{2+} regardless of its ligand field and n represents the number of equivalents of Pt^{2+} added per equivalent of G6-OH. In the present study, we examine DENs where n is 147. Second, the encapsulated metal ions are chemically reduced, which results in the formation of zero-valent DENs (G6-OH(Pt_{147})).

DENs have been characterized by a variety of techniques including UV−vis absorption spectroscopy,[5] transmission electron microscopy (TEM),[5] energy-dispersive X-ray spectroscopy (EDS),[13] X-ray photoelectron spectroscopy (XPS),[14] extended X-ray absorption fine structure (EXAFS),[4] and nuclear magnetic resonance (NMR).[15] One technique that has been used much less frequently is quasi-elastic light scattering (QLS, also known as dynamic light scattering),[16] which is an optical method for determining the diffusion coefficient—or equivalently, the hydrodynamic radius, R_h—of particles in solution.[17] QLS is not invasive, and it rapidly and precisely provides information about the effective particle size. Because it is an in situ method, QLS is also useful for measuring the kinetics of structural changes in solution. For example, by measuring the particle size as a function of solution conditions and time, it is possible to examine the mechanisms of oligomerization and aggregation.

Pt DENs are usually synthesized in aqueous basic solutions (pH ~10) at moderate salt concentration (~25 mM). Most studies of the size of DENs have been carried under these conditions, though their focus has usually been on the metal nanoparticles rather than the entire dendrimer/nanoparticle composite (DNC). Although a knowledge of the nanoparticle size is obviously important for practical applications (e.g., in catalysis), it is also useful to know the size of the composite (e.g., when DNCs are designed to penetrate cells as target-specific therapies).[18] Accordingly, it is important to explore the effect of different solution conditions on the size of these materials because they are large flexible molecules that may change conformation as a function of ionic strength or pH.[19,20]

In this article, we have used QLS to determine the size of DNCs at pH 10 and 7 and various salt concentrations and identities. The most interesting result of this study is that at pH 7 the size of the DNC composite is approximately double that at pH 10 (R_h ~ 8 nm vs 4 nm). Our results suggest that the DNC at pH 10 is a single dendrimer with a nanoparticle inside (a monomer) whereas the DNC at pH 7 is an aggregate of monomers. This aggregation occurs even though the positive charge in monomeric DNC increases as the pH is lowered.[21] Changes in ionic strength also alter the size of the DNCs, but to a much lesser degree. In contrast, the size of the nanoparticle-free dendrimer does not change with pH. The unexpected increase in the size of the composite is likely due to electrostatic interactions involving the encapsulated metal nanoparticle.

■ EXPERIMENTAL SECTION

Chemicals. G6-OH was purchased from Dendritech, Inc. (Midland, MI) as a 4.49% (w/v) methanol solution. Prior to use, the dendrimer stock solution was dried under vacuum and then was redissolved in HPLC-grade water to make a 200 μM solution (using the theoretical molecular weight of G6-OH). All solutions were prepared with HPLC-grade water (Fisher). K_2PtCl_4, K_2PdCl_4, $HAuCl_4$, $NaBH_4$, NaH_2PO_4, Na_2HPO_4, $NaBO_2$, $Na_2B_4O_7$, NaCl, NaF, and sodium citrate were purchased from Sigma-Aldrich and used as received.

Synthesis of DENs. Pt DENs were prepared using previously described methods.[4,7] Briefly, an aqueous 10.0 μM G6-OH dendrimer solution was combined with 147 equiv of a freshly prepared 0.1 M K_2PtCl_4 aqueous solution to yield $G6\text{-}OH(Pt^{2+})_{147}$. The solution was allowed to stir for 2 days to ensure the complexation of Pt^{2+} with the internal tertiary amines of the dendrimer. This metal ion–dendrimer complex was then reduced using a >10-fold molar excess of $NaBH_4$ from a freshly prepared aqueous 0.50 M stock solution. Reduction was allowed to proceed for 20 h in a sealed and stirred reaction vessel.

Au DENs were prepared using previously described methods.[22,23] Briefly, 147 equiv of $HAuCl_4$ per dendrimer was mixed with a 2.0 μM G6-OH solution. This solution was vigorously stirred for <2 min before the addition of the reducing agent, a 5-fold molar excess of $NaBH_4$ in 0.3 M NaOH.

Pd DENs were prepared using previously described methods.[6,24] In this case, a 10 μM G6-OH solution was stirred with 147 equiv of aqueous 0.10 M K_2PdCl_4. This solution was stirred for 15 min to allow complexation, and then a 10-fold molar excess of 1 M $NaBH_4(aq)$ solution was added as the reducing agent.

The G6-OH, $G6\text{-}OH(Pt^{2+})_{147}$, and $G6\text{-}OH(Pt_{147})$ solutions were exchanged with the solutions of interest by dialysis. Dialysis was carried out by placing 15 mL of the DEN solution into 12 kDa molecular weight cutoff dialysis sacks and suspending them in 4 L of the solution of interest. The dialysis solution was stirred for 24 h, after which aliquots were removed for subsequent analysis.

Characterization by UV–Vis and TEM. UV–vis measurements were made using a Hewlett-Packard 8453 spectrometer and 0.100 cm cells. An Orion pH meter with a Ross Sure-Flow pH electrode or a Hanna Instruments 1330 probe (Thermo Fisher Scientific, Waltham, MA) was used for pH measurements. All TEM images were recorded using a JEOL-2010F TEM operated at 200 kV. TEM samples were prepared by placing 7.0 μL of a 10.0 μM DEN solution on a carbon-coated Cu grid and then drying in air for at least 24 h. TEM size analysis was carried out using Digital Micrograph software. The width of the particle size distribution is reported to be $\pm 1\sigma$.

Quasi-Elastic Light Scattering (QLS). QLS measurements were performed on a home-built optical system that includes a 35 mW He–Ne laser (Coherent, Santa Clara, CA), a custom-made scattering cell (Precision Detectors, Bellingham, MA), and a PD2000DLS^{PLUS} 256 channel correlator (Precision Detectors, Bellingham, MA). The scattering angle was 90°, and all measurements were carried out at 20 $\pm$ 0.3 °C. The measured correlation functions were analyzed by a constrained regularization method as implemented in the Precision Deconvolve software (version 5.4) provided by Precision Detectors. This software computes the distribution of scattering intensity as a function of the diffusion coefficient. All samples were filtered through an Anotop 10 filter (0.02 μm; Whatman, Maidstone, U.K.) before being measured.

To convert the measured diffusion coefficient (D) to a hydrodynamic radius (R_h), the Stokes–Einstein relation was used:[17] $R_h = k_BT/6\pi\eta D$, where T is the temperature and η is the viscosity of the solution, which was taken to be that of water (1.002 mPa s). For the dilute solutions studied, this assumption introduces a systematic error in R_h of at most 3%. Because this error is almost always less than the statistical error in the average R_h, it was neglected.
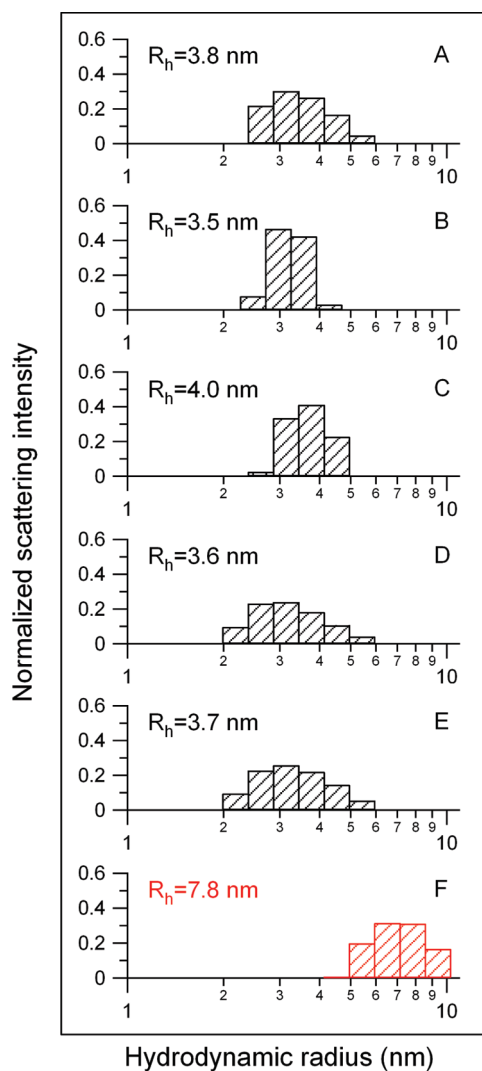
Figure 1. QLS data for (A) G6-OH at pH 10.2, (B) $G6\text{-}OH(Pt^{2+})_{147}$ at pH 9.2, (C) $G6\text{-}OH(Pt_{147})$ at pH 10.2, (D) G6-OH at pH 7.1, (E) $G6\text{-}OH(Pt^{2+})_{147}$ at pH 7.0, and (F) $G6\text{-}OH(Pt_{147})$ at pH 6.9.

The DENs absorb significantly at the wavelength of the He–Ne laser (633 nm). The resultant local heating changes the apparent value of R_h. To minimize heating effects, QLS measurements were made as a function of laser intensity, which was varied with neutral density filters of different optical densities (OD = 0.0, 0.5, 1.0, and 1.5). As expected, R_h increased as the intensity of the laser was reduced. Typically, the value of R_h was the same for the OD = 1.0 and 1.5 measurements, indicating that heating effects were not significant at these low intensities. The values of R_h reported are those for OD = 1.5; the averages presented are computed from the R_h distribution.

■ RESULTS AND DISCUSSION

Size Analysis by QLS: Fundamental Results. Figure 1 shows the average hydrodynamic radii and size distributions of G6-OH, $G6\text{-}OH(Pt^{2+})_{147}$, and $G6\text{-}OH(Pt_{147})$ at high and neutral pH. The Pt DENs are synthesized by reducing the $G6\text{-}OH(Pt^{2+})_{147}$ precursor at high pH and moderate ionic strength. For example, 25 mM $NaBH_4$ is used to reduce a 10 μM solution of $G6\text{-}OH(Pt^{2+})_{147}$, and the final pH of this solution is 10.2. Under

these conditions, the average R_h values of G6-OH (Figure 1A) and G6-OH(Pt$_{147}$) (Figure 1C) are essentially identical: R_h = 3.8 ± 0.1 and 4.0 ± 0.2 nm, respectively. The error in these measurements is reported as the statistical error in the average radius.

These R_h values are consistent with those expected on the basis of the molecular weight of G6-OH and G6-OH(Pt$_{147}$) if a globular structure is assumed.[25] These results are also consistent with NMR studies that show that the hydrodynamic radii of G6-OH and the corresponding Pd DNCs are the same at high pH (3.3 ± 0.3 nm).[15]

Interestingly, at pH 7, R_h for G6-OH(Pt$_{147}$) is about twice that of G6-OH (Figure 1F,D, respectively). Specifically, in 5 mM pH 7 phosphate buffer the average R_h for G6-OH(Pt$_{147}$) is 7.8 ± 0.4 nm, but it is just 3.6 ± 0.1 nm for G6-OH. Furthermore, whereas the scattering intensity is essentially constant for G6-OH as a function of pH, the scattering intensity for G6-OH-(Pt$_{147}$) at pH 7 is approximately double that at pH 10, which suggests that G6-OH(Pt$_{147}$) might not be in a monomeric form at pH 7.

To check whether the oxidation state of the metal affects the size of the particles, we measured R_h for the DEN precursor, G6-OH(Pt^{2+})$_{147}$, at different pH values. At high pH, the measured R_h for G6-OH(Pt^{2+})$_{147}$, R_h= 3.5 ± 0.2 nm, is close to that of G6-OH, R_h = 3.8 ± 0.1 nm (Figure 1B,A, respectively). At pH 7 (5 mM phosphate buffer), the precursor is also essentially the same size as G6-OH: R_h = 3.7 ± 0.2 nm and 3.6 ± 0.1 nm (Figure 1E,D, respectively). These results indicate that larger particles result only at neutral pH and in the presence of the zero-valent Pt DENs.

It is difficult to judge whether the polydispersities of the DNCs represented in Figure 1 are significantly different. This is because the widths of the distributions are determined by two factors: the true particle polydispersity in solution and the smoothing parameter of the regularization algorithm used to reconstruct the size distributions. Because the focus of this study is on the average R_h, we defer the discussion of the size distribution to future studies. Nevertheless, it is worth noting that the average R_h, which is determined to a precision of better than 5%, is much less sensitive to the value of the smoothing parameter than to the width of the true size distribution.[17] Thus, even though it is difficult to make quantitative comparisons of polydispersity, it is possible to make a quantitative comparison of the average R_h of the DNCs under different solution conditions.

Characterization by UV–Vis and TEM. Figure 2 shows the UV–vis spectra for G6-OH, G6-OH(Pt^{2+})$_{147}$, and G6-OH-(Pt$_{147}$) for undialyzed samples at pH 10 (except for G6-OH-(Pt^{2+})$_{147}$, which is at pH 9.2, the highest pH studied for this sample) and pH 7. These results are consistent with previously published data for these materials.[9] Specifically, G6-OH absorbs significantly in the range of 200–230 nm, and the G6-OH-(Pt^{2+})$_{147}$ precursor exhibits distinctive ligand-to-metal charge-transfer (LMCT) bands at ~220 and ~250 nm. For both G6-OH and G6-OH(Pt^{2+})$_{147}$, differences in the spectra at high pH and neutral pH are small. The spectrum for G6-OH(Pt$_{147}$) is composed of a monotonically decreasing absorbance at longer wavelengths and an LMCT peak at 250 nm, which corresponds to a small percentage of the unreduced precursor.[9] For the Pt DNCs, the difference between the absorbance at pH 10 and 7 is a little more pronounced. In particular, there is a small peak at 300 nm in the pH 7 sample that is not observed at pH 10. These
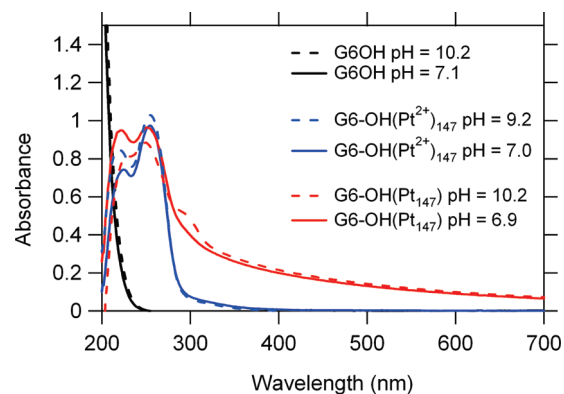
Figure 2. UV–vis absorbance spectra for G6-OH, G6-OH(Pt^{2+})$_{147}$, and G6-OH(Pt$_{147}$). G6-OH was used as a reference for G6-OH-(Pt^{2+})$_{147}$ and G6-OH(Pt$_{147}$); water was used as a reference for G6-OH.

differences might reflect a structural change that accompanies the formation of the large DNCs at pH 7.

The TEM results for the nanoparticles in the DNCs are shown in Figure 3. The average size of the nanoparticles does not depend on pH. The average diameter at pH 10 is 1.7 ± 0.4 nm, consistent with previous measurements for G6-OH(Pt$_{147}$).[9] At pH 7, the size of the DENs is essentially the same: 1.8 ± 0.4 nm. Thus, the formation of large DNCs does not affect the size of the nanoparticles within.

Size Analysis by QLS: Additional Solution Conditions. Our initial QLS results showed that large DNCs form in 5 mM phosphate buffer (pH 7) in the presence of metal nanoparticles. To investigate the generality of our findings, we determined the hydrodynamic radius of G6-OH(Pt$_{147}$) under a variety of solution conditions (Table 1). These results confirm that large DNCs form around neutral pH whereas at high pH the DNCs are much smaller, independent of the identity of the anions.

The ionic strength (I) also affects the size of the DNCs. For example, in 5 mM phosphate (pH 6.9, I = 10 mM), R_h = 7.8 ± 0.3 nm, whereas in 5 mM sodium citrate, which is at the same pH but at a higher ionic strength (pH 6.9, I = 30 mM), the size is significantly smaller: R_h = 6.2 ± 0.5 nm. The observation that both pH and I affect the size of DNCs suggests that electrostatic interactions are important in determining the solution behavior of DNCs. An extreme example of this is observed in deionized water. As the pH is lowered, the net positive charge of the dendrimer increases because of the protonation of the tertiary amines.[21] Thus, at sufficiently low ionic strength and weak electrostatic screening (i.e., when the Debye length, λ_D, is comparable to the average distance, d, between centers of DNCs) the repulsion between like-charged DNCs should lead to a larger diffusion coefficient and an apparently smaller radius (because $R_h \propto {}^1/_D$).[25,26] This expectation is observed experimentally: for a 10 μM solution of DNCs (d = 55 nm) at pH 7, the size in buffer-free water (R_h = 5.1 ± 0.6 nm, λ_D > 40 nm) is much smaller than in 5 mM phosphate buffer (R_h = 7.8 ± 0.3 nm, λ_D = 3.1 nm).

Electrostatic interactions, however, are not the only factors controlling the size of the DNCs. When the pH of a solution containing DNCs in 12.5 mM phosphate buffer is raised from 7.3 to 9.6 by the addition of OH$^-$, R_h remains essentially unchanged. Similarly, when NaCl or NaF is added to increase the ionic strength of a solution containing DNCs in 5 mM phosphate buffer, no change in size is observed. The inability to alter the size of DNCs formed at neutral pH demonstrates that the
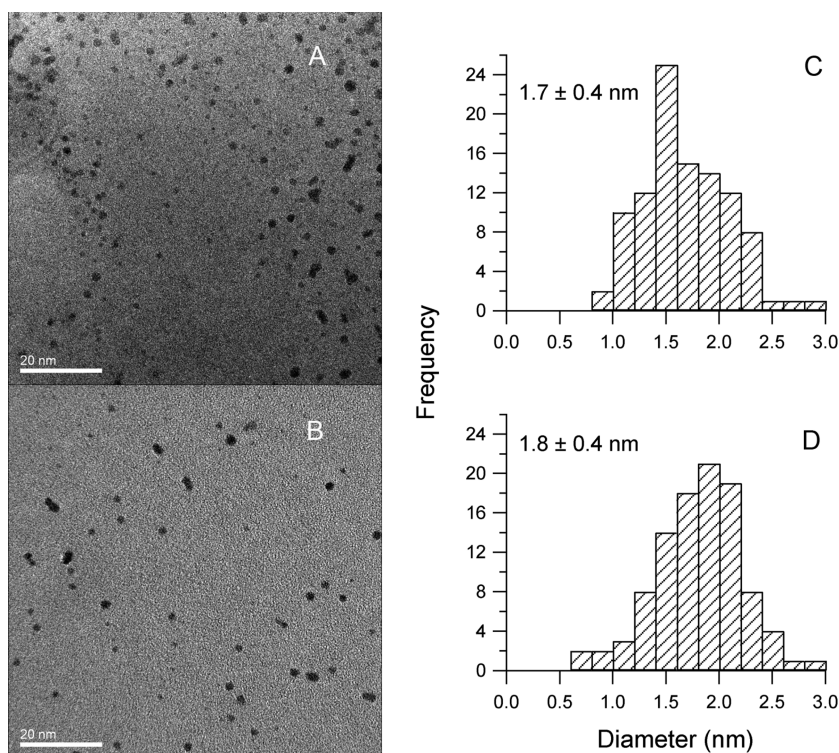
Figure 3. TEM images and histograms of particle sizes for Pt DNCs at (A, C) pH 10 and (B, D) pH 7.

Table 1. Hydrodynamic Radii for G6-OH(Pt$_{147}$)

solution	pH	I (mM)	R_h (nm)
25 mM borohydride/borate[a]	10.2	25	4.0 ± 0.2
10 mM borate	9.8	10	4.2 ± 0.2
12.5 mM tetraborate	9.1	~31	4.0 ± 0.2
10 mM sodium chloride	7.5	10	5.9 ± 0.2
12.5 mM phosphate	7.3	25	6.4 ± 0.3
12.5 mM phosphate + NaOH	9.6	~25	7.0 ± 0.2
5 mM phosphate	6.9	10	7.8 ± 0.3
5 mM phosphate + NaCl	6.8	25	8.1 ± 0.3
5 mM phosphate + NaF	6.8	25	8.1 ± 0.3
5 mM citrate	6.9	30	6.2 ± 0.5
deionized water	~7.2	<0.06	5.1 ± 0.6

[a] The initial solution is 25 mM sodium borohydride, which rapidly converts to borate.

Table 2. Hydrodynamic Radii for G6-OH as a Function of pH and Ionic Strength

solution	pH	I (mM)	R_h (nm)
25 mM borohydride/borate[a]	10.2	25	3.8 ± 0.1
10 mM borate	10.1	10	3.8 ± 0.1
12.5 mM tetraborate	9.3	~31	3.9 ± 0.1
10 mM sodium chloride	7.3	10	3.7 ± 0.1
12.5 mM phosphate	6.9	25	3.6 ± 0.1
5 mM phosphate	7.1	10	3.6 ± 0.1
5 mM citrate	7.6	30	3.8 ± 0.1
deionized water	~7.2	<0.06	3.0 ± 0.1

[a] The initial solution is 25 mM sodium borohydride, which rapidly converts to borate.

aggregation of DNCs is effectively irreversible, perhaps because of a structural change that occurs as the large DNCs form.

In contrast to the behavior of DNCs and consistent with previous findings, the sizes of G6-OH and G6-OH(Pt^{2+})$_{147}$ do not depend on pH or I (Tables 2 and 3).[20] For these species, R_h is essentially unchanged over a broad range of conditions, and the size is similar to that of the DNCs at high pH. The one exception to this observation is at very low ionic strength and low pH where, as with the DNCs, there is a large amount of intermolecular repulsion due to the protonated amines, leading to an apparently smaller radius.

Finally, our results are not unique to Pt DNCs. When the pH is decreased, Au and Pd DNCs also increase in size (Table 4).

Possible Mechanism for the Formation of Large DNCs.
The increase in R_h and the scattering intensity suggests that the large DNCs observed at pH 7 are aggregates of the monomeric DNCs present at pH 10. Any mechanism for the aggregation must explain the following observations: (i) aggregates form only at pH 7; (ii) reduced metal nanoparticles must be present; (iii) R_h depends on the ionic strength; and (iv) aggregates form irreversibly and are relatively stable (after their initial formation, additional aggregation is slow).

It is counterintuitive that more highly charged DNCs aggregate at pH 7 whereas uncharged DNCs at pH 10 do not. Accordingly, there must be a compensating attractive force, related to the nanoparticles themselves, that overcomes electrostatic repulsion. One possibility is that the dendrimers undergo a conformational change as a function of pH. Indeed, molecular

Table 3. Hydrodynamic Radii for G6-OH(Pt^{2+})$_{147}$ as a Function of pH and Ionic Strength

solution	pH	I (mM)	R_h (nm)
12.5 mM borate	9.2	~31	3.5 ± 0.2
10 mM sodium chloride	7.3	10	3.5 ± 0.1
5 mM phosphate	7.0	10	3.7 ± 0.2
5 mM citrate	7.5	30	3.6 ± 0.1
undialyzed	3.2	~4	3.1 ± 0.1

Table 4. Hydrodynamic Radii for G6-OH(Au$_{147}$) and G6-OH(Pd$_{147}$) as a Function of pH and Ionic Strength

solution	pH	I (mM)	R_h (nm)
2 μM G6-OH(Au$_{147}$) in 5 mM borohydride/borate[a]	10.6	5	3.2 ± 0.2
2 μM G6-OH(Au$_{147}$) in 5 mM phosphate	6.8	10	7.0 ± 0.2
20 μM G6-OH(Pd$_{147}$) in 50 mM borohydride/borate[a,b]	9.1	50	3.3 ± 0.3
10 μM G6-OH(Pd$_{147}$) in 5 mM phosphate	7.0	30	5.1 ± 0.5

[a] The initial solution is 25 mM sodium borohydride, which rapidly converts to borate. [b] From ref 15.

dynamics simulations have shown that as the pH is lowered, PAMAM dendrimers change from a dense core (with a maximum density at the dendrimer core and uniform void spacing) to a dense shell (with maximum density at the dendrimer periphery but nonuniform void spacings).[20]

The UV–vis results suggest that at pH 7 conformational changes may be occurring in the DNC. If this conformational change is of the type described above, then it could be the first step in the aggregation process. At pH 7, the more open structure of the dendrimer would allow for metal–metal association to occur if two nanoparticles come into close proximity. With this mechanism, the size of the aggregate would be determined by the competition among electrostatic repulsion, entropic effects (which would keep the DNCs apart), and metal–metal attraction. This mechanism would also allow for different sizes as a function of ionic strength because the change in the Debye length would affect the electrostatic interaction energy.[27]

Another puzzle is related to the size and scattering intensity of the DNCs. Both the size and intensity can be used independently to estimate the aggregation number. If the large species at pH 7 (R_h ~8 nm) is assumed to be an aggregate composed of n identical DNCs (those found at pH 10, R_h ~4 nm), then the doubling of the hydrodynamic radii corresponds to n in the range of 4 to 6 (the hydrodynamic radius of a dimer would be 1.4 times that of a monomer).[28] In principle, because both the metal nanoparticles and the dendrimer are much smaller than the wavelength of the light used (633 nm), they can be treated as Rayleigh scatterers.[29] In this regime, if n monomers assemble to form an aggregate, then $I_{olig} = nI_{mon}$, where I_{mon} is the scattering intensity from a solution of monomers and I_{olig} is the scattering intensity from the assembled aggregates.[17] Therefore, in our case, the scattering intensity of the large DNCs at pH 7 should be 4 to 6 times that of the small DNCs at pH 10. Instead, we find that the scattering intensity increases at most by a factor of 2. This

discrepancy is not due to different amounts of absorption because the absorbance at 633 nm is essentially independent of pH (Figure 2). It may be that part of the size increase is due to the swelling of individual dendrimers. This swelling would not significantly change the scattering intensity because the particles, even when swollen, would still be much smaller than the wavelength of the light used.[29] Alternatively, the interactions between the metal nanoparticles lead to non-Rayleigh scattering even though the nanoparticles are very small.

SUMMARY AND CONCLUSIONS

We have determined the sizes of G6-OH(Pt$_{147}$) DNCs, the G6-OH(Pt^{2+})$_{147}$ precursors, and G6-OH empty dendrimers using QLS at high and neutral pH for various salt concentrations and identities. At neutral pH, the hydrodynamic radius of the DNC is approximately double that at high pH, and the sizes of the empty dendrimers and DNC precursors do not change with pH. Changes in ionic strength also alter the size of the DNCs but do not affect the size of the DNC precursor and empty dendrimer unless the ionic strength is very low. Importantly, these results are highly reproducible.

We suggest that the unexpected increase in the size of DNCs is probably due to aggregate formation driven by electrostatic interactions involving the metal nanoparticles. This aggregation occurs even though the positive charge on the monomeric DNC increases as the pH is lowered. Further work will define the details of this aggregate and may present a new way to control the size of DNCs in solution.

AUTHOR INFORMATION

Corresponding Author
*(R.M.C.) E-mail: crooks@cm.utexas.edu. Phone: 512-475-8674. (N.A.) E-mail: asherie@yu.edu. Phone: 212-960-5452.

ACKNOWLEDGMENT

REFERENCES

(1) Sardar, R.; Funston, A. M.; Mulvaney, P.; Murray, R. W. Langmuir 2009, 25, 13840–13851.
(2) Garcia-Martinez, J. C.; Lezutekong, R.; Crooks, R. M. J. Am. Chem. Soc. 2005, 127, 5097–5103.
(3) Knecht, M. R.; Crooks, R. M. New J. Chem. 2007, 31, 1349–1353.
(4) Knecht, M. R.; Weir, M. G.; Myers, V. S.; Pyrz, W. D.; Ye, H. C.; Petkov, V.; Buttrey, D. J.; Frenkel, A. I.; Crooks, R. M. Chem. Mater. 2008, 20, 5218–5228.
(5) Scott, R. W. J.; Wilson, O. M.; Crooks, R. M. J. Phys. Chem. B 2005, 109, 692–704.
(6) Wilson, O. M.; Knecht, M. R.; Garcia-Martinez, J. C.; Crooks, R. M. J. Am. Chem. Soc. 2006, 128, 4510–4511.
(7) Ye, H. C.; Crooks, R. M. J. Am. Chem. Soc. 2005, 127, 4930–4934.

(8) Ye, H. C.; Crooks, R. M. *J. Am. Chem. Soc.* **2007**, *129*, 3627–3633.

(9) Knecht, M. R.; Weir, M. G.; Frenkel, A. I.; Crooks, R. M. *Chem. Mater.* **2008**, *20*, 1019–1028.

(10) Chung, Y. M.; Rhee, H. K. *J. Mol. Catal.* **2003**, *206*, 291–298.

(11) Lang, H. G.; Maldonado, S.; Stevenson, K. J.; Chandler, B. D. *J. Am. Chem. Soc.* **2004**, *126*, 12949–12956.

(12) Ozturk, O.; Black, T. J.; Perrine, K.; Pizzolato, K.; Williams, C. T.; Parsons, F. W.; Ratliff, J. S.; Gao, J.; Murphy, C. J.; Xie, H.; Ploehn, H. J.; Chen, D. A. *Langmuir* **2005**, *21*, 3998–4006.

(13) Jin, L.; Yang, S. P.; Wu, H. X.; Huang, W. W.; Tian, Q. W. *J. Appl. Polym. Sci.* **2008**, *108*, 4023–4028.

(14) Qiu, L. M.; Liu, F.; Zhao, L. Z.; Yang, W. S.; Yao, J. N. *Langmuir* **2006**, *22*, 4480–4482.

(15) Gomez, M. V.; Guerra, J.; Myers, V. S.; Crooks, R. M.; Velders, A. H. *J. Am. Chem. Soc.* **2009**, *131*, 14634–14635.

(16) Kavitha, M.; Parida, M. R.; Prasad, E.; Vijayan, C.; Deshmukh, P. C. *Macromol. Chem. Phys.* **2009**, *210*, 1310–1318.

(17) Lomakin, A.; Teplow, D. B.; Benedek, G. B. Quasielastic Light Scattering for Protein Assembly Studies. In *Amyloid Proteins: Methods and Protocols*; Sigurdsson, E. M., Ed.; Methods in Molecular Biology; Humana Press: Totowa, NJ, 2005; Vol. 299, pp 153−173.

(18) Shi, X. G.; Wang, S. H.; Meshinchi, S.; Van Antwerp, M. E.; Bi, X. D.; Lee, I. H.; Baker, J. R. *Small* **2007**, *3*, 1245–1252.

(19) Liu, Y.; Chen, C. Y.; Chen, H. L.; Hong, K. L.; Shew, C. Y.; Li, X.; Liu, L.; Melnichenko, Y. B.; Smith, G. S.; Herwig, K. W.; Porcar, L.; Chen, W. R. *J. Phys. Chem. Lett.* **2010**, *1*, 2020–2024.

(20) Liu, Y.; Bryantsev, V. S.; Diallo, M. S.; Goddard, W. A. *J. Am. Chem. Soc.* **2009**, *131*, 2798–2799.

(21) Niu, Y. H.; Sun, L.; Crooks, R. A. *Macromolecules* **2003**, *36*, 5725–5731.

(22) Garcia-Martinez, J. C.; Crooks, R. M. *J. Am. Chem. Soc.* **2004**, *126*, 16170–16178.

(23) Kim, Y. G.; Oh, S. K.; Crooks, R. M. *Chem. Mater.* **2004**, *16*, 167–172.

(24) Niu, Y. H.; Yeung, L. K.; Crooks, R. M. *J. Am. Chem. Soc.* **2001**, *123*, 6840–6846.

(25) Schmitz, K. S. *An Introduction to Dynamic Light Scattering by Macromolecules*; Academic Press: New York, 1990.

(26) Prinsen, P.; Odijk, T. *J. Chem. Phys.* **2007**, *127*, 115102.

(27) Tsonchev, S.; Schatz, G. C.; Ratner, M. A. *Chem. Phys. Lett.* **2004**, *400*, 221–225.

(28) Garcia de la Torre, J.; Bloomfield, V. A. *Q. Rev. Biophys.* **1981**, *14*, 81–139.

(29) Kerker, M. *The Scattering of Light and Other Electromagnetic Radiation*; Academic Press: New York, 1969.